COO-2218-26
29 January 1975

Ionization and Charge Exchange Rate Coefficients for CTR Calculations*

by

Ronald L. Miller

and

George H. Miley

Nuclear Engineering Program
University of Illinois at Urbana-Champaign
Urbana, Illinois 61801

* This work was performed under the auspices of the Energy Research and Development Administration under Contract AT(11-1)2218

DISCLAIMER

Ionization and Charge Exchange Rate Coefficients for CTR Calculations

Abstract: Microscopic collisional ionization and charge exchange cross sections for neutral, hydrogenic atoms in CTR plasmas are averaged over plasma phase-space distribution functions to obtain <σv> rate coefficients. Prior calculations of this type were restricted to isotropic plasma distributions with injection at an energy near the mean plasma energy, however, in the present case, mirror loss-cone distributions are allowed. A discussion of methods and exemplary results in the energy range [0.1 - 300 keV] are presented.

1. Introduction

Studies involving the transport of neutral test particles in background plasmas require knowledge of the microscopic cross sections for the various interaction processes (e.g. electron-atom collisional ionization, ion-atom collisional ionization and ion-atom charge exchange).* If, as is often the case, the speeds of the plasma particles are comparable to the test particle speed, it is necessary to average the cross sections over the plasma phase space distribution to obtain the $\langle \sigma v \rangle$ rate coefficients for the interaction processes.

The formal definition of the rate coefficient begins by considering the distributions of two distinct particle species in 3-D phase space.[1] The first particle species has the number density n_1 and the velocity distribution $f_1(\vec{v}_1)$ such that the number of these particles in an incremental element $d\vec{v}_1$ is given by $n_1 f_1(\vec{v}_1) d\vec{v}_1$. These particles will interact with a number $n_2 f_2(\vec{v}_2) d\vec{v}_2$ of the second particle species in the element $d\vec{v}_2$ at the rate

$$dR = n_1 f_1(\vec{v}_1) n_2 f_2(\vec{v}_2) \; |\vec{v}_1 - \vec{v}_2| \; \sigma(|\vec{v}_1 - \vec{v}_2|) \; d\vec{v}_1 d\vec{v}_2 \qquad (1)$$

where $|\vec{v}_1 - \vec{v}_2|$ is the relative speed of the two interacting particles and $\sigma(|\vec{v}_1 - \vec{v}_2|)$ is the microscopic cross section (assumed to be functionally dependent upon the relative speed) for the reaction process under consideration.

The total reaction rate, R, is the sixfold integral over all space, viz.,

---

* Other processes (e.g. excitation and scattering) will not be considered here.

$$R = n_1 n_2 \int_{\vec{v}_1, \vec{v}_2} f_1(\vec{v}_1)\ f_2(\vec{v}_2)\ |\vec{v}_1 - \vec{v}_2|\ \ \sigma(|\vec{v}_1 - \vec{v}_2|)\ d\vec{v}_1 d\vec{v}_2 \qquad (2)$$

The multiple integral in the above expression may be interpreted as the interaction cross section averaged over the entire range of relative speeds, suitably weighted according to the distributions $f_1(\vec{v}_1)$ and $f_2(\vec{v}_2)$. This quantity is called the rate coefficient, $\langle\sigma v\rangle$, which is defined as follows

$$\langle\sigma v\rangle \equiv \int_{\vec{v}_1,\ \vec{v}_2} f_1(\vec{v}_1)\ f_2(\vec{v}_2)\ |\vec{v}_1 - \vec{v}_2|\ \ \sigma(|\vec{v}_1 - \vec{v}_2|)\ d\vec{v}_1 d\vec{v}_2 \qquad (3)$$

Now the reaction rate may conveniently expressed as the product of the number densities of the dissimilar particles and the reaction coefficient, namely

$$R = n_1 n_2 \langle\sigma v\rangle \qquad (4)$$

This should, of course, be consistent with the familiar form

$$R = \psi_1 \Sigma \qquad (5)$$

where ψ_1 is a flux of test particles incident upon a target population with macroscopic cross section Σ. Equation (4) may be cast in the form

$$R = n_1 n_2 \langle\sigma v\rangle \frac{v_1}{v_1} \qquad (6)$$

which, under the usual definition, $\psi_1 \equiv n_1 v_1$, becomes

$$R = \psi_1 n_2 \frac{\langle\sigma v\rangle}{v_1} \qquad (7)$$

Thus, a generalized expression for the macroscopic interaction cross section is seen to be

$$\Sigma = n_2 \frac{\langle\sigma v\rangle}{v_1} \qquad (8)$$

It may be remarked that in the cold plasma limit of $v_2 \ll v_1$, $\langle \sigma v \rangle$ reduces to σv_1 and the reaction rate again becomes

$$R = \psi_1 n_2 \sigma = \psi_1 \Sigma \tag{9}$$

as required by Equation (5).

2. Calculation of generalized rate coefficients

In order to apply the formal definition of the general rate coefficient presented as Equation (3) above, it is necessary to perform some further manipulations. Consider a test particle characterized by the velocity distribution $f_1(\vec{v}_1)$ as it travels through and interacts with a population of field particles with the distribution $f_2(\vec{v}_2)$. For a test particle with speed, v_t, and angular orientations, ϕ_t, and $\mu_t \equiv \cos\theta_t$, using the Dirac delta function and spherical coordinate system, the normalized test particle velocity distribution is

$$f_1(\vec{v}_1) = \frac{1}{v_1^2} \delta(v_1 - v_t)\ \delta(\phi_1 - \phi_t)\ \delta(\mu_1 - \mu_t) \tag{10}$$

The relative speed, $|\vec{v}_1 - \vec{v}_2|$, of the test particle and a field particle is given by

$$v_R \equiv |\vec{v}_1 - \vec{v}_2| = [v_1^2 + v_2^2 - 2v_1 v_2 \cos\gamma]^{1/2} \tag{11}$$

where γ is the angle between the two particles' velocity vectors and is given by

$$\gamma = \cos^{-1}[\mu_1\mu_2 + \sqrt{1-\mu_1^2}\ \sqrt{1-\mu_2^2}\cos(\phi_1 - \phi_2)]\ . \tag{12}$$

The incremental phase space elements are defined as follows

$$d\vec{v}_1 \equiv v_1^2 dv_1 d\phi_1 d\mu_1 \tag{13a}$$

$$d\vec{v}_2 \equiv v_2^2 dv_2 d\phi_2 d\mu_2 \tag{13b}$$

Using Equations (10-13), Equation (3) may be rewritten in the form

$$\langle \sigma v \rangle = \int_{\mu_1=-1}^{+1} \int_{\phi_1=0}^{2\pi} \int_{v_1=0}^{\infty} \int_{\mu_2=-1}^{+1} \int_{\phi_2=0}^{2\pi} \int_{v_2=0}^{\infty} \frac{1}{v_1^2} \delta(v_1 - v_t)\, \delta(\phi_1 - \phi_t)\, \delta(\mu_1 - \mu_t)$$

$$\times\ f_2(\vec{v}_2)\, [v_1^2 + v_2^2 - 2v_1 v_2 \cos\gamma]^{1/2}\, \sigma(v_R)\, v_1^2\, v_2^2$$

$$\times\ dv_2 d\phi_2 d\mu_2 dv_1 d\phi_1 d\mu_1 \tag{14}$$

This expression may be readily integrated over the subscript "1" variables using the sifting property of the Dirac delta function to obtain

$$\langle \sigma v \rangle = \int_{\mu_2=-1}^{+1} \int_{\phi_2=0}^{2\pi} \int_{v_2=0}^{\infty} f_2(\vec{v}_2)\, [v_t^2 + v_2^2 - 2v_t v_2 \cos\Gamma]^{1/2} \sigma(v_R)\, v_2^2$$

$$\times\ dv_2 d\phi_2 d\mu_2 \tag{15}$$

where, from Equation (12), it is seen that

$$\Gamma = \cos^{-1}[\mu_t \mu_2 + \sqrt{1-\mu_t^2}\ \sqrt{1-\mu_2^2}\, \cos(\phi_t - \phi_2)] \tag{16}$$

and the cross section is evaluated such that

$$\sigma(v_R) = \sigma(|\vec{v}_t - \vec{v}_2|) \tag{17}$$

It remains to characterize both the field particle velocity distribution function, $f_2(\vec{v}_2)$, and the interaction cross sections of interest as analytic expressions. These issues will be considered in later sections of this report. Also, Equation (15) must be normalized such that

$$\int_{-1}^{+1}_{\mu_2} \int_{0}^{2\pi}_{\phi_2} \int_{0}^{\infty}_{v_2} f_2(\vec{v}_2)\, v_2^2\, dv_2 d\phi_2 d\mu_2 = 1 \qquad (18)$$

It is expected that Equation (15) will require evaluation by multi-dimensional numerical integration, although, under favorable simplifying circumstances, a closed form solution might be obtainable.

3. Cross section data

Following Riviere,[2] analytic expressions for the collisional ionization and charge exchange cross sections are obtained. It is assumed (with some justification[3]) that the cross sections for interactions between hydrogenic isotopes depend only on the relative collision speed and not on the masses of the particles involved. The expressions cited by Riviere cast the cross sections as functions of the collision energy, E, where $E = \frac{1}{2} m_2 v_R^2$. Values for E are in eV units throughout.

The following expressions are used for the ionization of atomic hydrogen by protons

$$\sigma_{ii}(E) = 3.6 \times 10^{-12} E^{-1} \log_{10}(0.1666E) \text{ for } E > 1.5 \times 10^5 \text{eV} \quad \text{cm}^2 \qquad (19a)$$

$$\log_{10}\sigma_{ii}(E) = -0.8712(\log_{10}E)^2 + 8.156(\log_{10}E) - 34.833$$
$$\text{for } E < 1.5 \times 10^5 \text{eV} \qquad (19b)$$

The microscopic cross section for charge exchange by protons in atomic hydrogen is fairly well represented by the following expression

$$\sigma_{cx}(E) = \frac{0.6937 \times 10^{-14}(1 - 0.155 \log_{10}E)^2}{1 + 0.1112 \times 10^{-14}E^{3.5}} \quad \text{cm}^2 \qquad (20)$$

This expression is found to be somewhat less reliable in representing experimental results in low energy (< 100eV) and high energy (>1.0 x 10^5eV) extrapolations; in both cases Equation (20) over-estimates the available data.

The above cross section expressions are presented in Figure 1 as a function of deuterium atom impact energy, E. Figure 2 graphs the product of the impact speed, v_t, and the microscopic interaction cross sections as a function of impact energy, E, for deuterium atoms incident upon deuterium ions. It will be remembered that this represents the limiting case for rate coefficients in a cold plasma, and as such will be used to test the numerical results discussed in later sections of this report.

4. Plasma velocity distribution functions

Equation (15) requires an expression for the plasma velocity distribution function, $f_2(\vec{v}_2)$. Following Holdren[4], it is assumed that the distribution function is azimuthally invariant and approximately separable in the μ and v components of velocity; μ being the cosine of the angle, θ, between the plasma velocity vector and the local magnetic field vector, $\vec{B}$, and v being the speed of the plasma particle. Thus, to first order in angle,

$$f_2(\vec{v}_2) \propto \frac{1}{v_2^2} f(v_2)\, M(\mu) \qquad (21)$$

where $M(\mu)$ is the lowest eigenmode of Legendre's equation

$$(1 - \mu^2)\frac{d^2M}{d\mu^2} - 2\mu\frac{dM}{d\mu} + \lambda M = 0 \tag{22}$$

$$|\mu| \leq 1,\ M(\mu \geq \mu_0) = 0,\ M(\mu) = M(-\mu)$$

For application to mirror devices, $\mu_0 = [(R' - 1)/R']^{1/2} = \cos\theta_0$, where θ_0 is the critical loss-cone angle. Particles whose velocity vectors are within θ_0 of $\vec{B}$ escape preferentially from the system. R' is the effective mirror ratio in the presence of an ambipolar potential, Φ, defined such that

$$R' = R(1 + 2Ze\Phi/mv_z^2)^{-1} \tag{23}$$

where R is the vacuum mirror ratio.

In mirror devices, the velocity distribution of electrons is assumed to be in approximate equilibrium, following Riviere, allowing use of a Maxwellian speed distribution and the default isotropic case, $M(\mu)=1$, corresponding to $R'=\infty$. Maxwellian, isotropic distribution are assumed for both ions and electrons in toroidal devices.

For ions in mirror devices, the following expression (normalized to be unity at $\mu = 0$) is used for the first normal-mode angular distribution

$$M(\mu) = \frac{\mu_0^2 - \mu^2 + (3\mu_0^2 - 1)\log_e[(1 - \mu^2)/(1 - \mu_0^2)]}{\mu_0^2 - (3\mu_0^2 - 1)\log_e[1 - \mu_0^2]} \tag{24}$$

For convenience in some applications, this expression may be approximated[5] to within 10% by

$$M(\mu) = 1 - \mu^2/\mu_0^2, \text{ for } R' < 1.5 \tag{25a}$$

$$M(\mu) = 1 + \log_e(1 - \mu^2)/\log_e R', \text{ for } R' > 1.5 \tag{25b}$$

Equation (24) was used for the numerical computation of mirror rate coefficients discussed below. The behavior of Equation (24) is shown

for two typical mirror ratios, $R' = 3$, 10, in Figure (3).

In mirror devices, loss-cone effects and particle injection at energy E_o distort the energy distribution function of confined ions. The expected steady-state ion energy distribution functions for mirror ratios $R' = 3$ and 10 have been computed using Fokker-Planck techniques by Kuo-Petravic and coworkers.[6] The following analytical expressions, having the same functional forms (but with modified coefficients) as suggested by Riviere[2], are used to represent these energy distributions.

for $R' = 3$, and $0.18 < E/E_o < 1.0$

$$f(E/E_o) = -1.316(E/E_o)^2 + 2.831(E/E_o) - 0.515 \qquad (26a)$$

for $R' = 3$, and $1.0 < E/E_o < 2.5$

$$f(E/E_o) = 1.52 - 0.95[-3.69 + 5(E/E_o) - (E/E_o)^2]^{1/2} \qquad (26b)$$

for $R' = 10$, and $0.05 < E/E_o < 1.0$

$$f(E/E_o) = 1.00 - 1.4251[0.85 - (E/E_o)]^2 \qquad (27a)$$

for $R' = 10$, and $1.0 < E/E_o < 2.5$

$$f(E/E_o) = 1.52 - 0.95[-3.69 + 5(E/E_o) - (E/E_o)^2]^{1/2} \qquad (27b)$$

These new expressions more closely reproduce the desired energy distribution shapes.

An equilibrium Maxwellian energy distribution function with $kT = E_o$ and scaled such that

$$f(E/E_o) = 1.45(E/E_o)^{1/2} \exp(-E/E_o) \qquad (28)$$

is graphed for comparison with Equations (26-27) in Figure 4.

In order to make the integrations over these energy distributions compatible with Equation (15), it is necessary to apply the transformation

$$\int_{(E/E_o)_{min}}^{(E/E_o)_{max}} f(E/E_o)\, d(E/E_o) = \int_{v_{min}}^{v_{max}} f(v^2/v_o^2)\, \frac{2v}{v_o^2}\, dv \qquad (29)$$

where $E_o = \frac{1}{2} m_2 v_o^2$. Inspection of Figure (4) suggests the following values for the limits of integration in Equation (29) for the mirror loss-cone distributions

$$(E/E_o)_{min} = 0.18, \text{ for } R' = 3 \qquad (30a)$$

$$= 0.04, \text{ for } R' = 10 \qquad (30b)$$

$$(E/E_o)_{max} = 2.5, \text{ for both } R' = 3,10 \qquad (30c)$$

5. Numerical Computation of Rate Coefficients

A FORTRAN program called MCSAV2 has been developed which numerically integrates Equation (15). The program has been implemented on the IBM 360/75 machine operated by the University of Illinois Digital Computer Laboratory. A three-dimensional version of the Gauss-Legendre quadrature technique is used to perform the required integrations. This method requires that a standard variable transformation of the form

$$F(x) = (b-a)\, F[a + (b-a)t]\, dt \qquad (31)$$

be applied to each of the phase-space dimensions in order that the integrations over the intervals [a,b] may be more conveniently performed over the unit interval [0,1].

Such data as mirror ratio; test and field particle identities; test particle velocity vector and magnetic field vector orientations; and plasma energy are set at the user's option. Specifications of either Maxwellian or mirror energy distributions and either isotropic or loss-cone angular distributions are also made. Program results are presented in tabular form as functions of test particle speed and kinetic energy. Once such rate coefficient tables are available for a series of representative parameters spanning the regimes of interest, an interpolation scheme may be employed to approximate intermediate values not themselves obtained by actual integration.

6. Discussion of Results

The rate coefficient results reported by Riviere are restricted to cases involving isotropic plasma angular distributions and test particle kinetic energies equal to the characteristic energy, E_o, of the background plasma. By relaxing these restrictions it is possible to obtain more general results for application to neutral particle transport studies in CTR plasmas. A series of runs of the MCSAV2 code have been made, the results of which are included with this report to suggest those features of rate coefficient behavior that are of potential consequence to CTR design studies. While the results presented in Figures (5-7) are primarily of interest to energetic neutral beam injection analyses, extrapolation of the curves to low ($<10^3$ eV) test particle kinetic energies gives rate coefficients applicable to neutral particles expected in CTR devices to enter the plasma either from first wall reflux or surrounding neutral gas blankets.[7]

Figures (5a-b) present charge exchange and ionization rate coefficients calculated according to Equation (15) above for neutral deuterium test particles in a background of deuterium ions having the Maxwellian distribution of Equation (28) and an isotropic ($M(\mu)=1$) angular distribution. E_o, the

characteristic energy of the background distribution is varied as a parameter for representative values in the range [0.1 - 300.0 keV]. In Figures (6a-b), the Maxwellian speed distribution has been replaced by the R' = 3 mirror loss-cone speed distribution of Equation (26) above. The isotropic angular distribution has been retained. The new speed distribution produces non-trivial changes in the resultant rate coefficients, suggesting the desirability of accurate representations of the plasma distributions used in neutral particle transport calculations. As expected, for very energetic test particles (i.e. those whose kinetic energy greatly exceeds E_o) the influence of the distributed plasma background becomes small and the rate coefficients tend to converge toward an asymptotic limit.

Figures (7a-e) present rate coefficient results for a plasma background with fixed energy E_o = 65 keV. This energy corresponds to the operating energy of the proposed mirror Fusion Engineering Research Facility (FERF).[8] These results incorporate the combined effects of the loss-cone speed distribution and the anisotropic loss-cone angular distribution. The effective mirror ratio is again equal to 3. The angle, θ_i, between the test particle velocity vector and the $\vec{B}$-field is varied over its range $[0,\pi/2]$. Figure (8) plots these same charge exchange results as a function of injection angle for various deuterium test particle energies. The striking feature of this series of results is the clear variation with angle in the charge exchange rate coefficients, particularly in the range of test particle energies consistent with energetic neutral-beam injection for eventual mirror fusion devices. Near-perpendicular injection tends to maximize the probability of particle charge exchange. Physically, if the test particle velocity vector lies in or near the phase space loss-cone of the background plasma, there are fewer plasma ions available whose velocity vectors are compatible with the low collision speed

bias of the charge exchange cross section exhibited in Figure 1. These various effects are being incorporated into a Monte Carlo computer simulation of neutral beam injection for the FERF device,[9] which should provide the desired extension of previous work[10] in this area.

Some additional effort was expended in order to verify the results of the above calculations. As a check, the equations used by Riviere, which employ a formalism somewhat different from that described in Section 2 of this report, were programmed in order to replicate the results of the generalized MCSAV2 code under the default case of an isotropic target plasma distribution. For sufficiently energetic D° test particles, both approaches were found to return the cold plasma limit results predicted by Figure (2). Confirmation of results for higher values of E_o is also obtained. Finally, the modifications mentioned in Section 4 to Riviere's analytic expression for the plasma loss-cone energy distributions were found to have only minor influence on the rate coefficient results.

7. Electron Ionization

In most plasmas of CTR interest, collisions between the neutral test particle and the background electrons can also result in ionization of the neutral atom. The cross section for collisional ionization of hydrogen atoms by electron impact can be represented by the analytic expression,

$$\sigma_{ei}(E_o) = \frac{6.513 \times 10^{-14}}{U_i^2} \; g(x) \; cm^2 \qquad (32)$$

where $U_i \equiv$ ionization potential (13.6 eV)

$x \equiv$ the ratio E_o/U_i

and $g(x) \equiv \frac{1}{x}\left(\frac{x-1}{x+1}\right)^{3/2}\left[1 + \frac{2}{3}\left(1 - \frac{1}{2x}\right) \log_e(2.7 + \sqrt{x-1})\right]$

The electrons are assumed to have a Maxwellian energy distribution characterized by $kT_e = E_o$. Since the mean electron speed in usual applications is so much greater than typical neutral test particle speeds, the rate coefficients for the electron case are found to be essentially constant functions of test particle speed. The format of previous figures is therefore abandoned and ionizational rate coefficients are plotted in Figure (9) as a function of electron energy E_o. The broken line represents results of the MCSAV2 code while the solid line is a simple analytic approximation to Riviere's results given by

$$\langle \sigma v \rangle_{ei} \approx 0.4877228\ E_o^{(-0.3467852)} \qquad (cm^3/sec) \qquad (33)$$

This approximation to the MCSAV2 results breaks down in the low energy (< 1 keV) extrapolation but is considered adequate for CTR design studies, for which the electron energy usually is at least a few keV.

8. Conclusion

The availability of charge exchange and ionization rate coefficients tailored to specific applications allows the development of more sophisticated neutral particle transport models for such CTR applications as energetic neutral beam injection or neutral gas blanketing. The accompanying results indicate the variations and sensitivities which make detailed knowledge of these rate coefficients important. The techniques required to obtain these generalized results are seen to be straightforward and easily incorporated into overall plasma transport codes.

Acknowledgment: Encouragement and support by Drs. R. J. Burke and T. A. Coultas while one of us (RLM) was a summer employee of the Engineering Division of Argonne National Laboratory as well as stimulating discussion with Dr. G. A. Carlson of Lawrence Livermore Laboratory are gratefully acknowledged.

Figure Captions

Figure 1 Deuterium ionization and charge-exchange microscopic cross sections as a function of impact energy. These curves are obtained from Equations (19-20) of this report.

Figure 2 Product of the impact speed and deuterium ionization and charge-exchange microscopic cross sections as a function of impact energy. These curves represent the cold plasma limiting cases for the respective interaction rate coefficients.

Figure 3 Angular component of the mirror loss-cone plasma phase-space distribution function vs. μ, the cosine of the angle θ from the magnetic axis, for two typical effective mirror ratios, i.e. $R' = 3,10$; obtained from Equation (24) of this report.

Figure 4 Energy component of the mirror loss-cone and Maxwellian plasma space distribution functions as obtained from Equations (26-28) of this report.

Figure 5a-b Deuterium-Deuterium charge exchange and ionization interaction rate coefficients as a function of neutral test particle kinetic energy for a plasma with a Maxwellian, isotropic phase space distribution for various values of E_o.

Figure 6a-b Deuterium-Deuterium charge exchange and ionization interaction rate coefficients as a function of neutral test particle kinetic energy for a $R' = 3$ mirror-confined plasma having an isotropic angular distribution for various values of E_o.

Figure 7a-e Deuterium-Deuterium charge exchange and ionization interaction rate coefficients as a function of neutral test particle kinetic energy for a $R' = 3$ mirror-confined plasma with $E_o = 65$ keV for various values of injection angle Θ_i in the range $[0, \pi/2]$.

Figure 8 Deuterium-Deuterium charge exchange interaction rate coefficients as a function of injection angle Θ_i for various values of injection energy in a $R' = 3$ mirror-confined plasma with $E_o = 65$ keV.

Figure 9 Comparison of electron-Deuterium ionization interaction rate coefficient results as obtained from Equation (15) of this report to the approximation given by Equation (33) of this report.

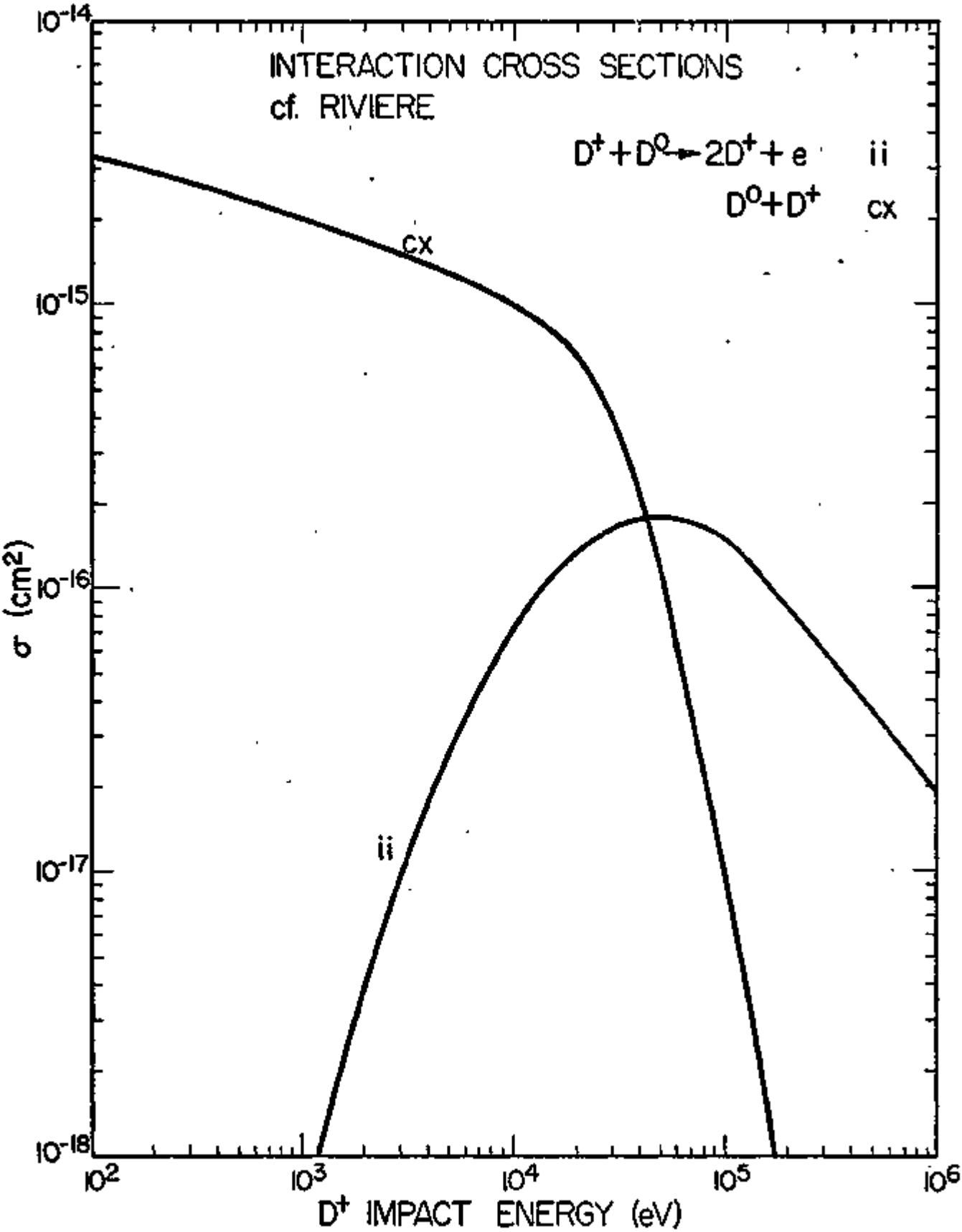
INTERACTION CROSS SECTIONS
cf. RIVIERE
$D^+ + D^0 \rightarrow 2D^+ + e$ ii
$D^0 + D^+$ cx
cx
ii
10^{-14}
10^{-15}
10^{-16}
10^{-17}
10^{-18}
σ (cm^2)
10^2
10^3
10^4
10^5
10^6
D^+ IMPACT ENERGY (eV)

Figure 1

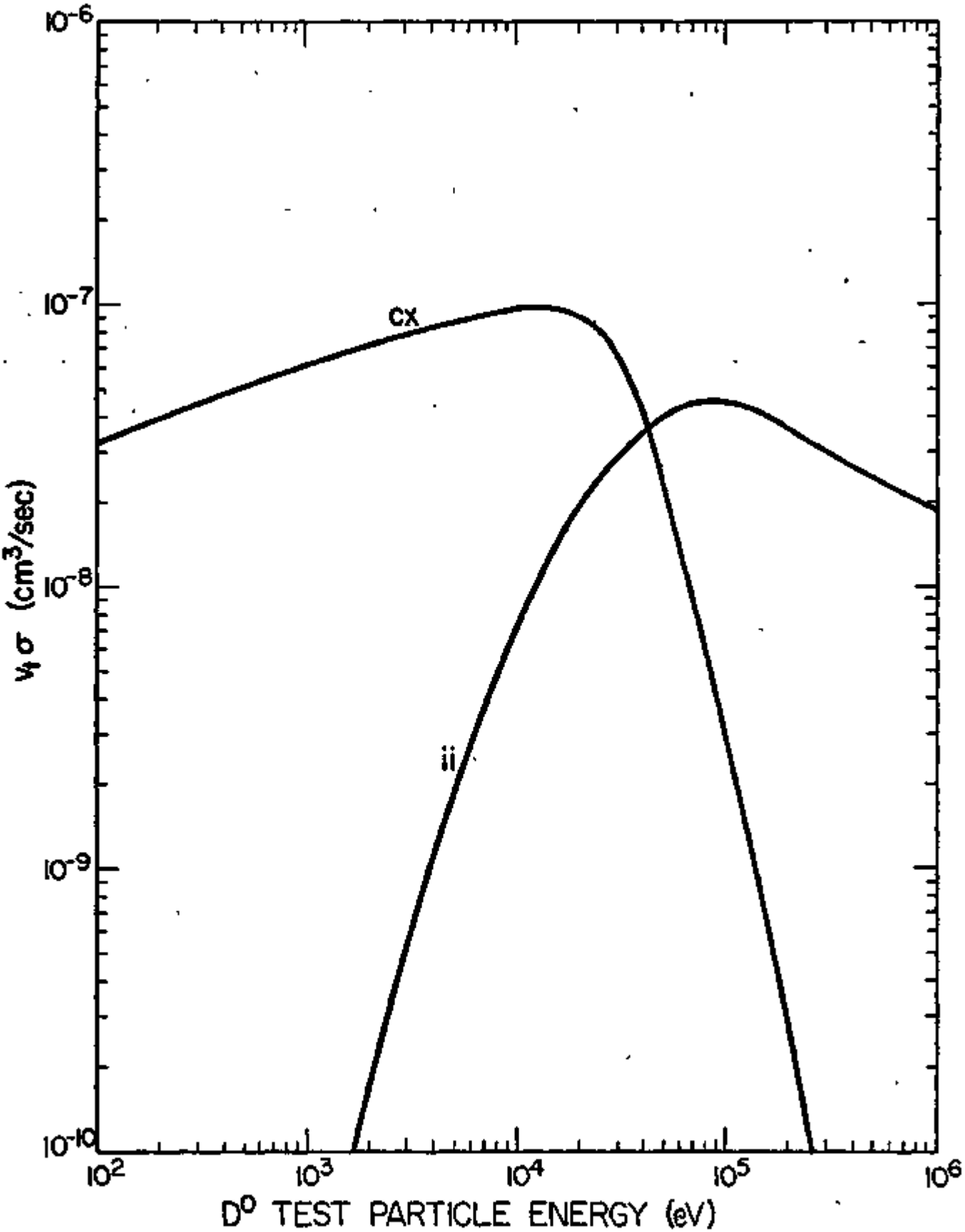
10^{-6}
10^{-7}
10^{-8}
10^{-9}
10^{-10}
$v_i \sigma$ (cm^3/sec)
CX
ii
10^2
10^3
10^4
10^5
10^6
D^0 TEST PARTICLE ENERGY (eV)

Figure 2

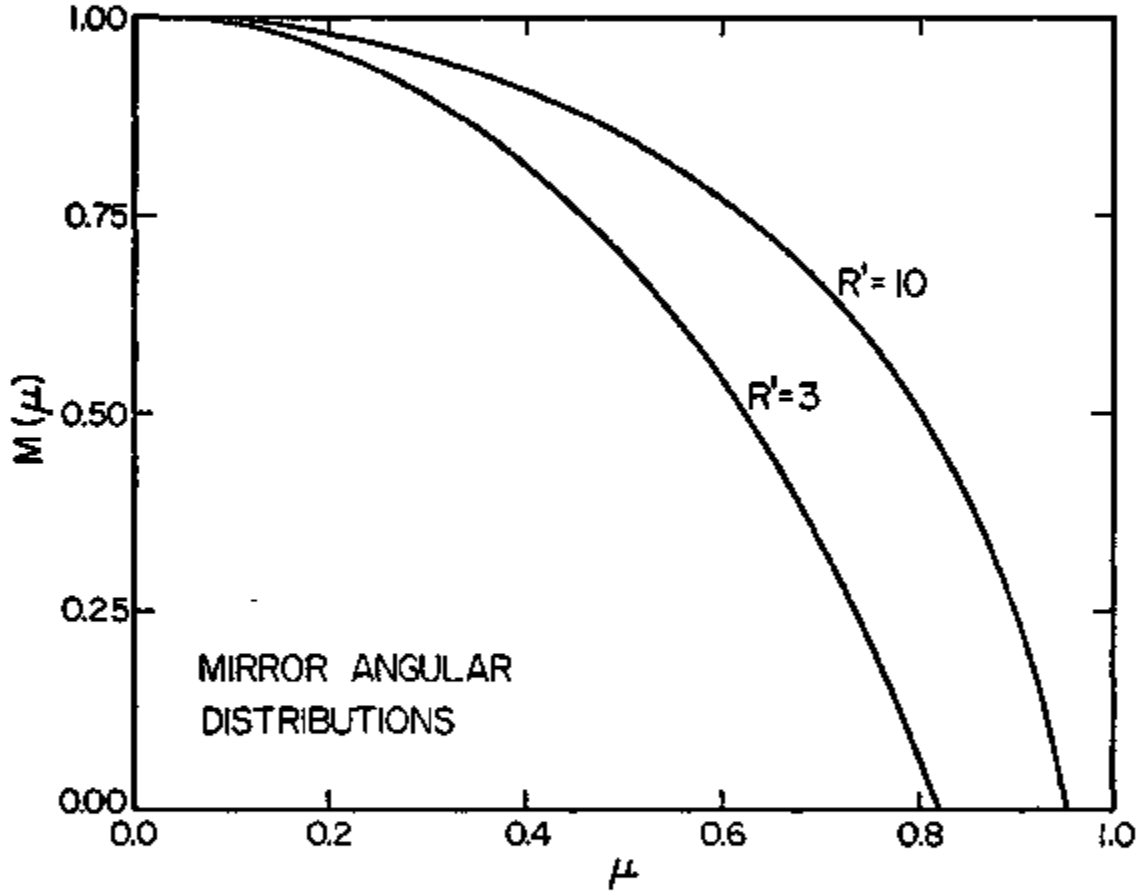
1.00
0.75
0.50
0.25
0.00
M (μ)
R'= 10
R'=3
MIRROR ANGULAR
DISTRIBUTIONS
0.0
0.2
0.4
0.6
0.8
1.0
μ

Figure 3

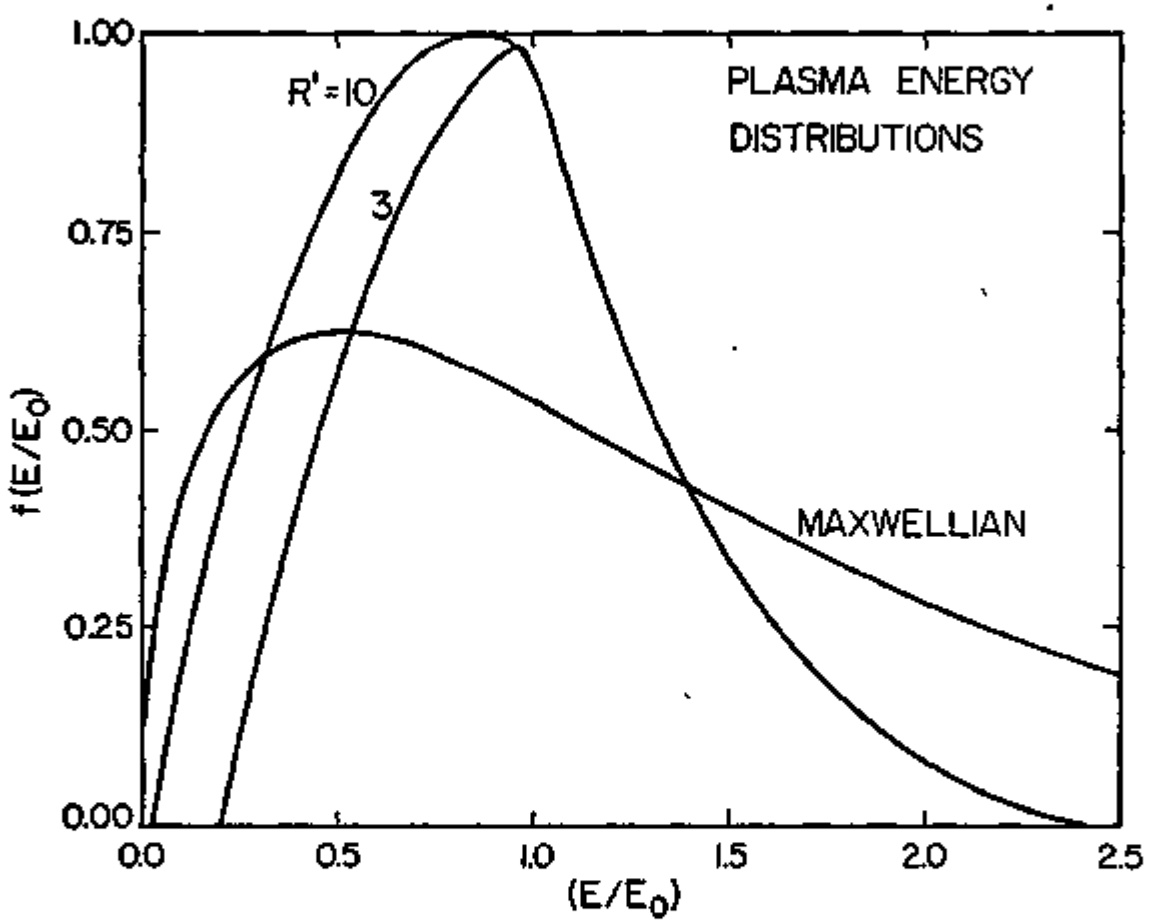
PLASMA ENERGY
DISTRIBUTIONS
R' = 10
3
MAXWELLIAN
f(E/E0)
(E/E0)
1.00
0.75
0.50
0.25
0.00
0.0
0.5
1.0
1.5
2.0
2.5

Figure 4

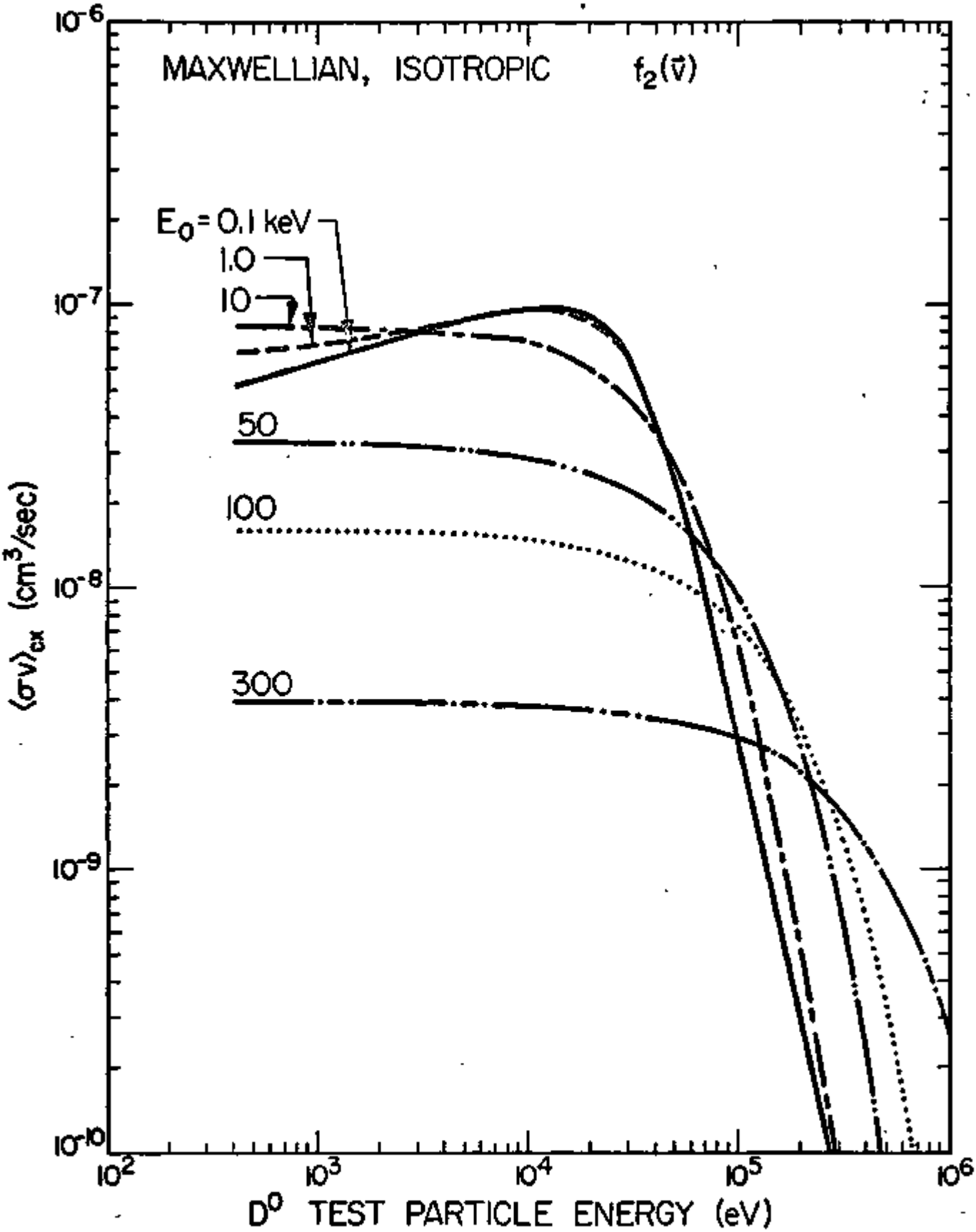
MAXWELLIAN, ISOTROPIC $f_2(\vec{v})$
E_0 = 0.1 keV
1.0
10
50
100
300
10^{-6}
10^{-7}
10^{-8}
10^{-9}
10^{-10}
$(\sigma v)_{cx}$ (cm^3/sec)
10^2
10^3
10^4
10^5
10^6
D^0 TEST PARTICLE ENERGY (eV)

Figure 5a

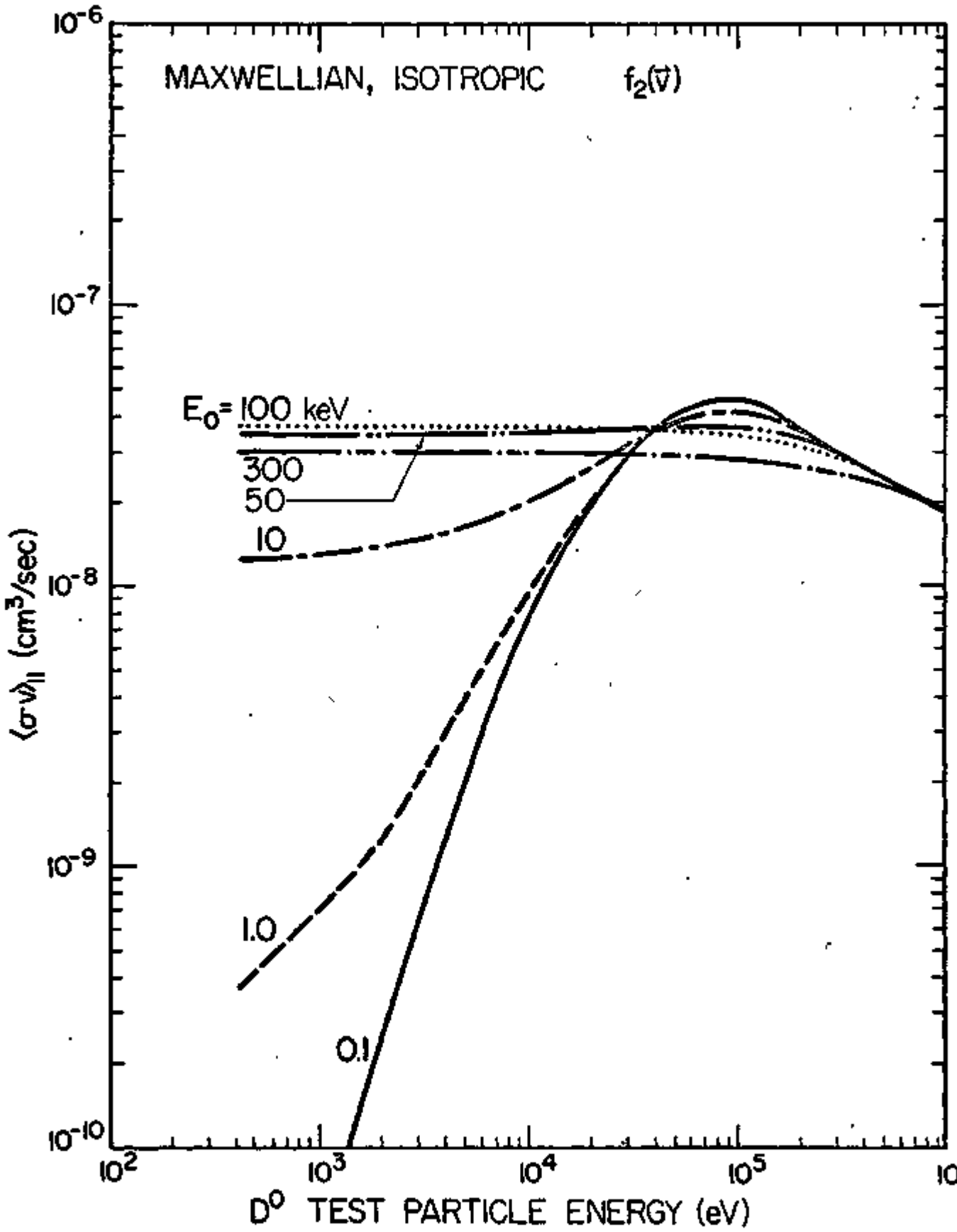
MAXWELLIAN, ISOTROPIC $f_2(\vec{v})$
E_0= 100 keV
300
50
10
1.0
0.1
$\langle\sigma v\rangle_{11}$ (cm^3/sec)
10^{-6}
10^{-7}
10^{-8}
10^{-9}
10^{-10}
10^2
10^3
10^4
10^5
10^6
D^0 TEST PARTICLE ENERGY (eV)

Figure 5b

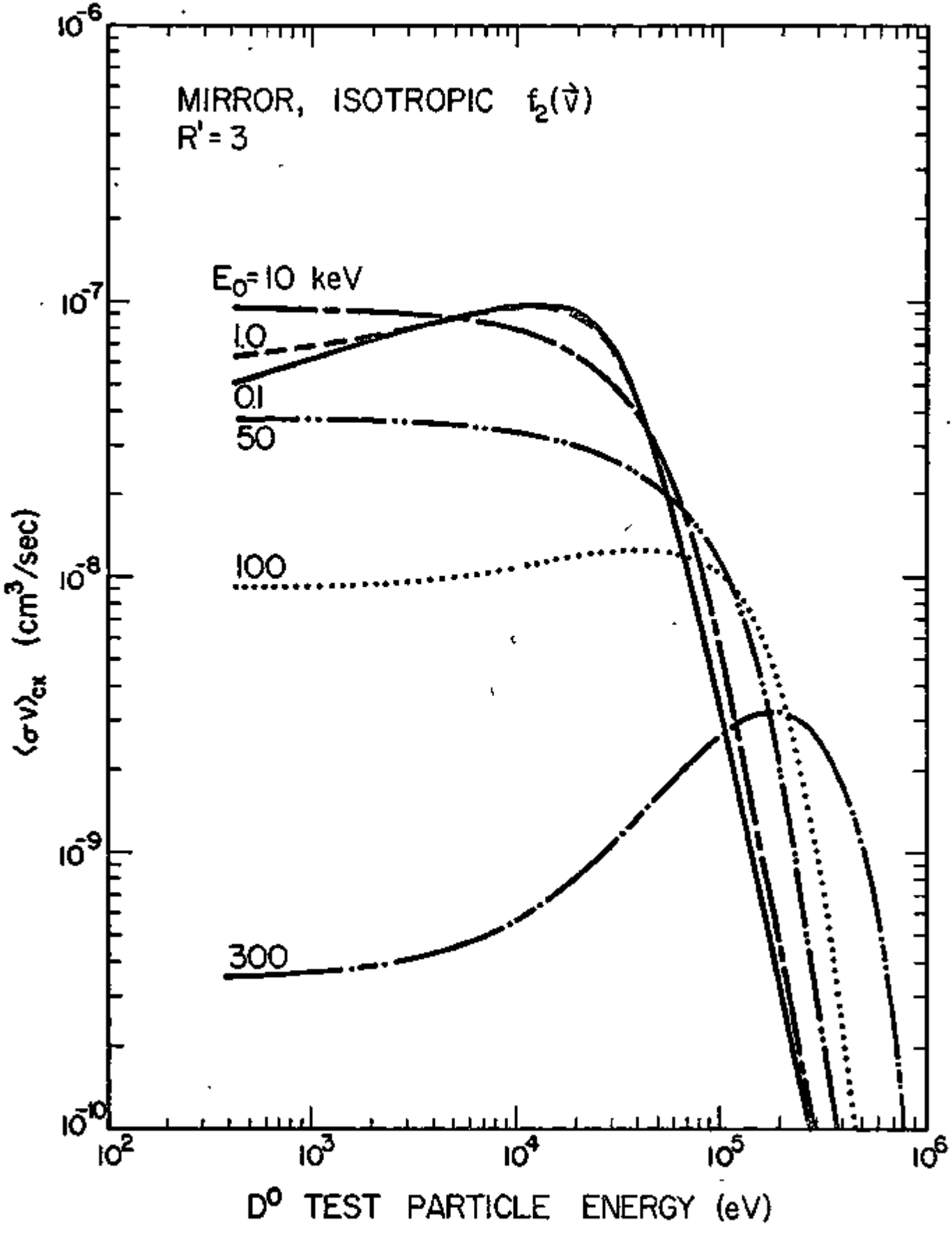
MIRROR, ISOTROPIC $f_2(\vec{v})$
R' = 3
E_0= 10 keV
10
0.1
50
100
300
$(\sigma v)_{cx}$ (cm^3/sec)
10^{-6}
10^{-7}
10^{-8}
10^{-9}
10^{-10}
10^2
10^3
10^4
10^5
10^6
D^0 TEST PARTICLE ENERGY (eV)

Figure 6a

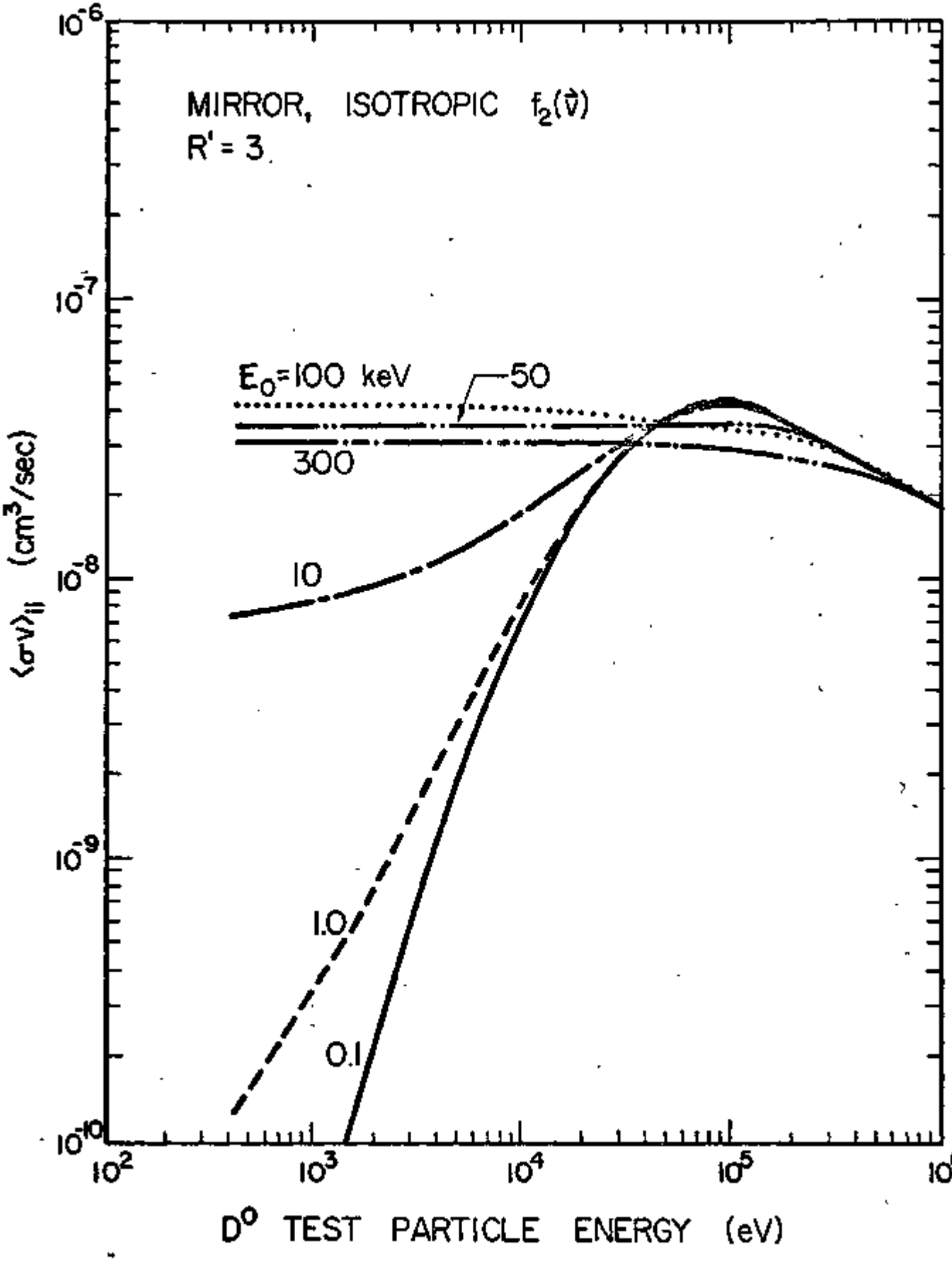
MIRROR, ISOTROPIC $f_2(\vec{v})$
R' = 3
E_0=100 keV
50
300
10
1.0
0.1
$\langle\sigma v\rangle_{11}$ (cm^3/sec)
10^{-6}
10^{-7}
10^{-8}
10^{-9}
10^{-10}
10^2
10^3
10^4
10^5
10^6
D^0 TEST PARTICLE ENERGY (eV)

Figure 6b

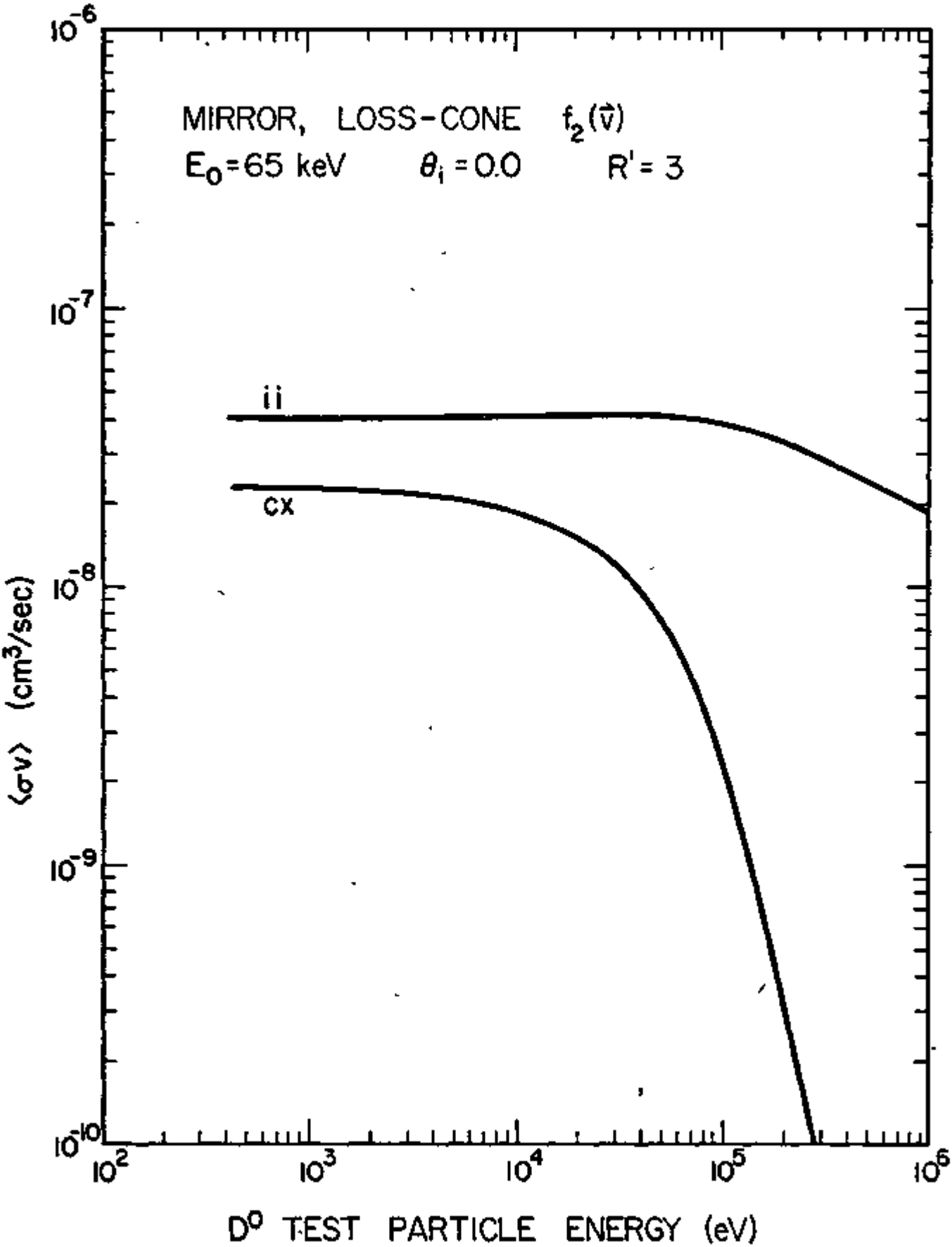
MIRROR, LOSS-CONE $f_2(\vec{v})$
E_0=65 keV θ_i = 0.0 R' = 3
ii
cx
$\langle\sigma v\rangle$ (cm^3/sec)
10^{-6}
10^{-7}
10^{-8}
10^{-9}
10^{-10}
10^2
10^3
10^4
10^5
10^6
D^0 TEST PARTICLE ENERGY (eV)

Figure 7a

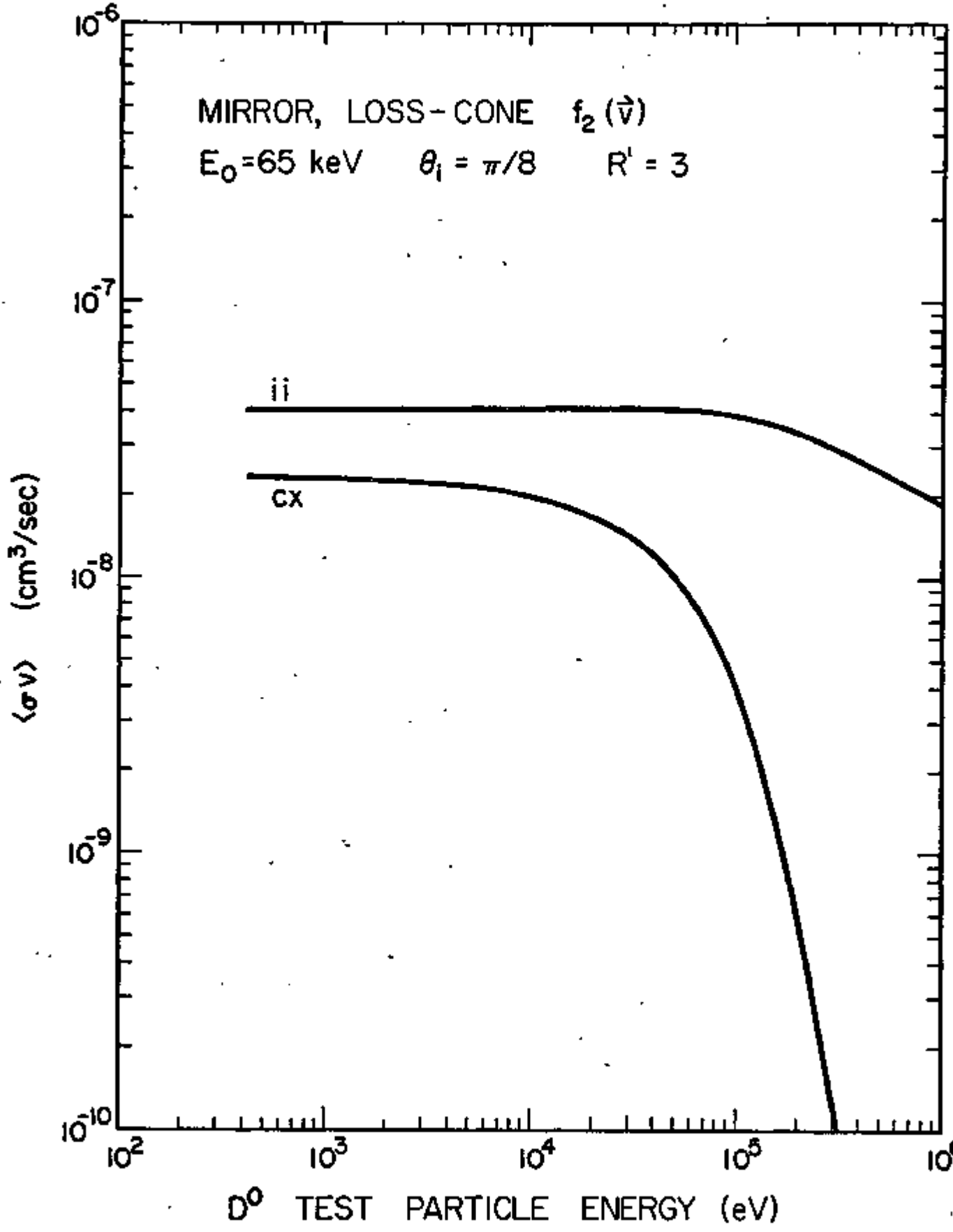
MIRROR, LOSS-CONE $f_2(\vec{v})$
E_0=65 keV $\theta_i = \pi/8$ $R' = 3$
ii
cx
$\langle\sigma v\rangle$ (cm^3/sec)
10^{-6}
10^{-7}
10^{-8}
10^{-9}
10^{-10}
10^2
10^3
10^4
10^5
10^6
D^0 TEST PARTICLE ENERGY (eV)

Figure 7b

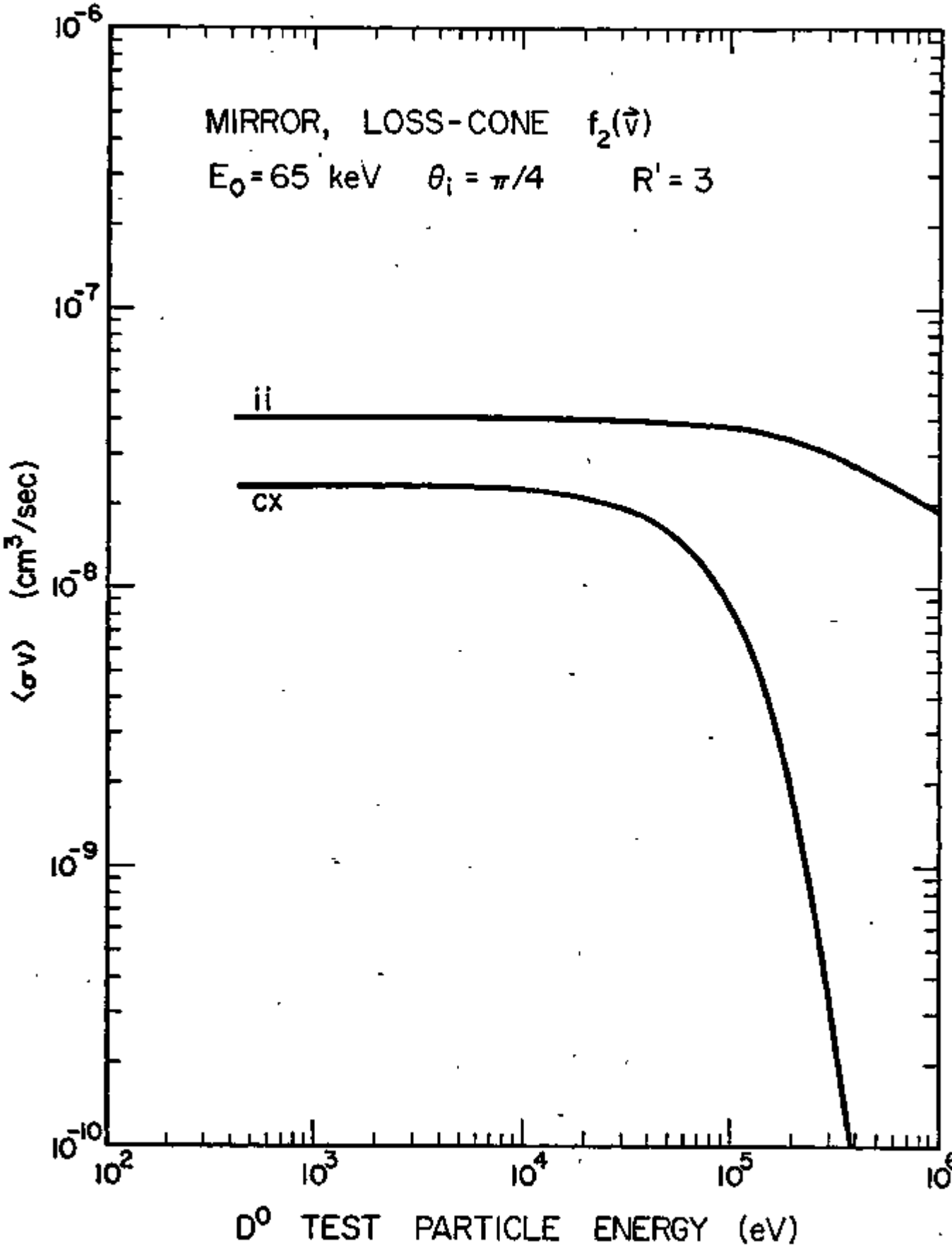
MIRROR, LOSS-CONE $f_2(\vec{v})$
$E_0 = 65$ keV $\theta_i = \pi/4$ $R' = 3$
ii
cx
$\langle \sigma v \rangle$ (cm^3/sec)
10^{-6}
10^{-7}
10^{-8}
10^{-9}
10^{-10}
10^2
10^3
10^4
10^5
10^6
D^0 TEST PARTICLE ENERGY (eV)

Figure 7c

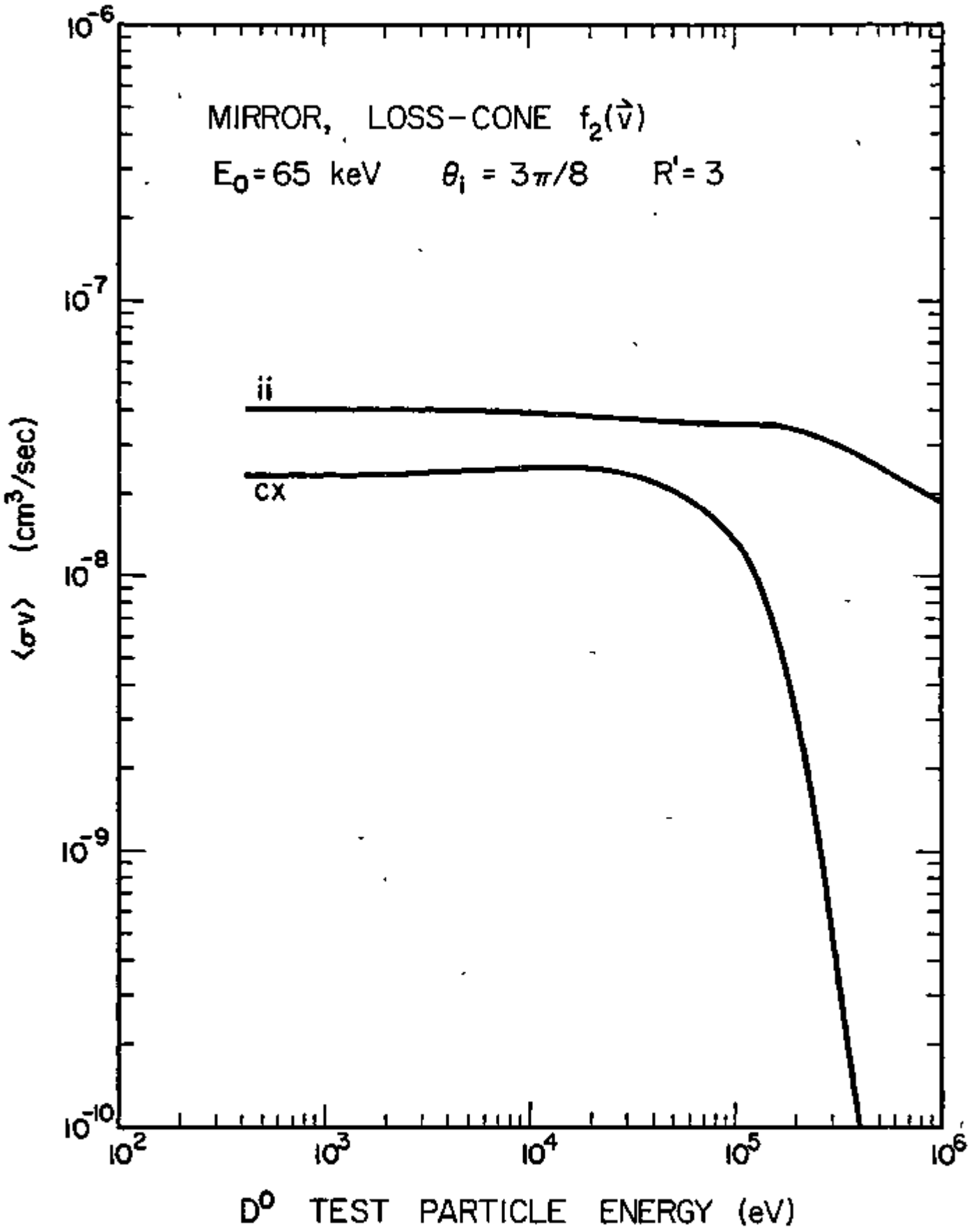
MIRROR, LOSS-CONE $f_2(\vec{v})$
$E_0 = 65$ keV $\theta_i = 3\pi/8$ $R' = 3$
ii
cx
$\langle\sigma v\rangle$ (cm^3/sec)
10^{-6}
10^{-7}
10^{-8}
10^{-9}
10^{-10}
10^2
10^3
10^4
10^5
10^6
D^0 TEST PARTICLE ENERGY (eV)

Figure 7d

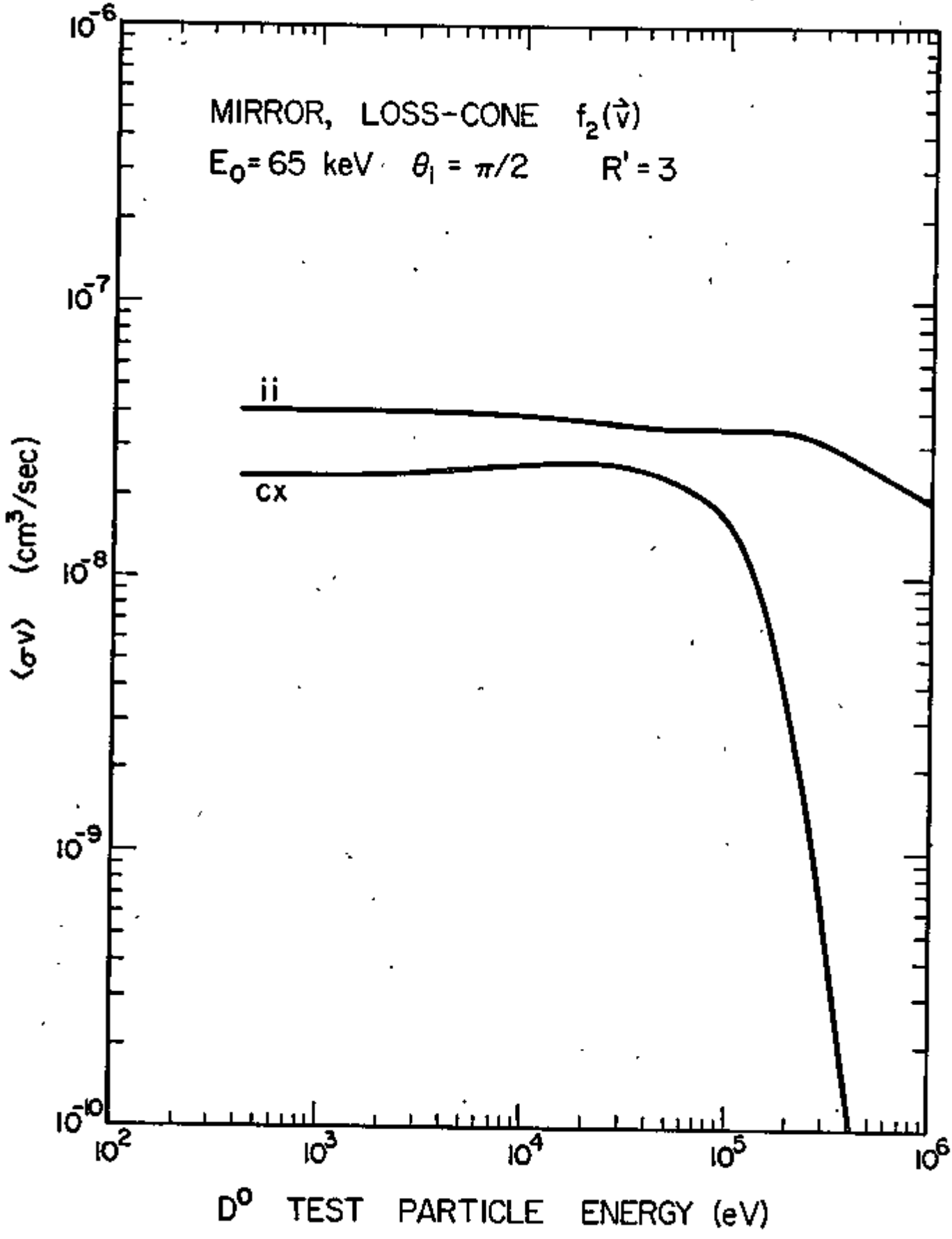
MIRROR, LOSS-CONE $f_2(\vec{v})$
E_0= 65 keV $\theta_1 = \pi/2$ R' = 3
ii
cx
10^{-6}
10^{-7}
10^{-8}
10^{-9}
10^{-10}
(σv) (cm^3/sec)
10^2
10^3
10^4
10^5
10^6
D^0 TEST PARTICLE ENERGY (eV)

Figure 7e

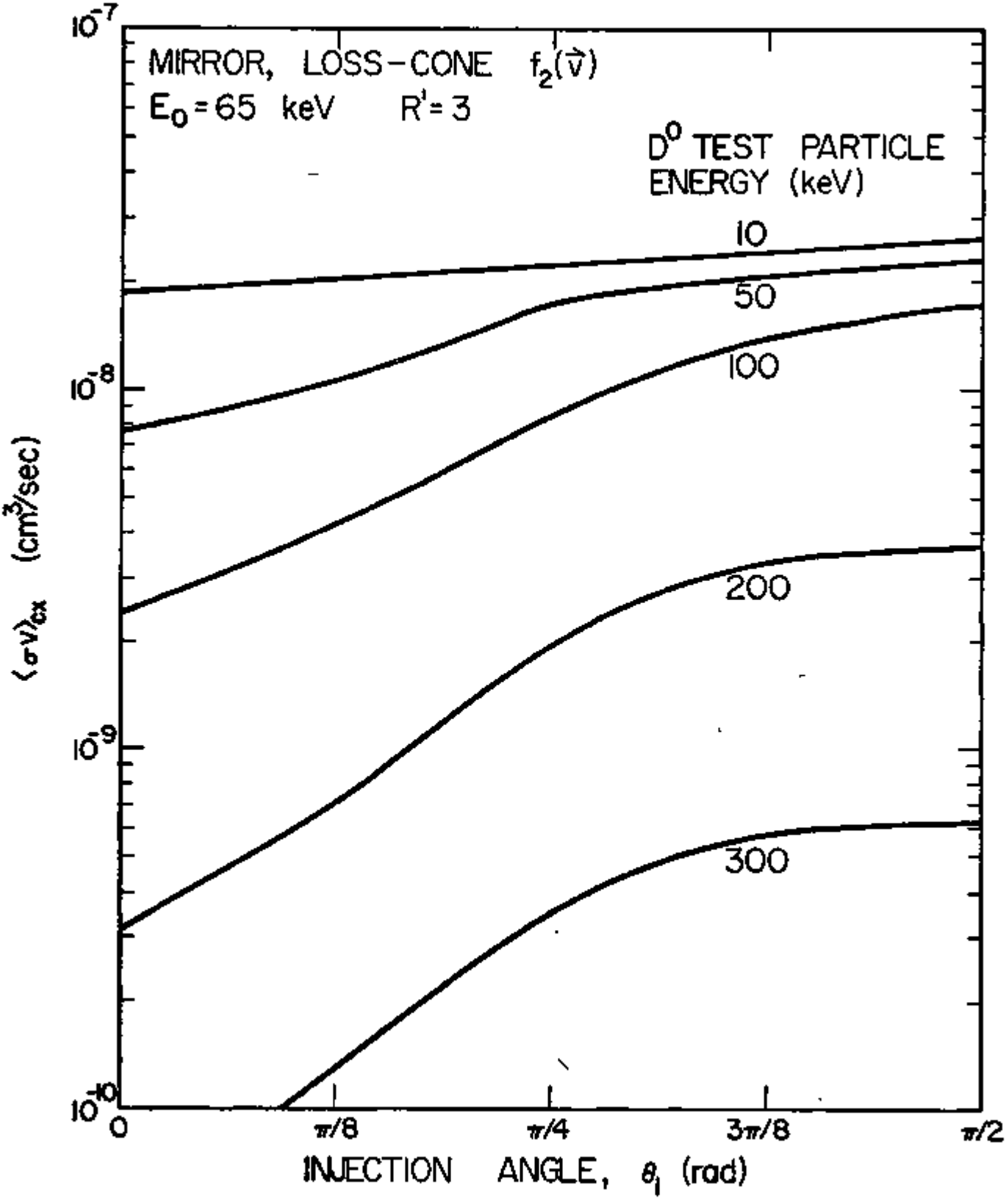
MIRROR, LOSS-CONE $f_2(\vec{v})$
$E_0 = 65$ keV $R' = 3$
D^0 TEST PARTICLE ENERGY (keV)
10
50
100
200
300
10^{-7}
10^{-8}
10^{-9}
10^{-10}
$(\sigma v)_{ex}$ (cm^3/sec)
0
$\pi/8$
$\pi/4$
$3\pi/8$
$\pi/2$
INJECTION ANGLE, θ_i (rad)

Figure 8

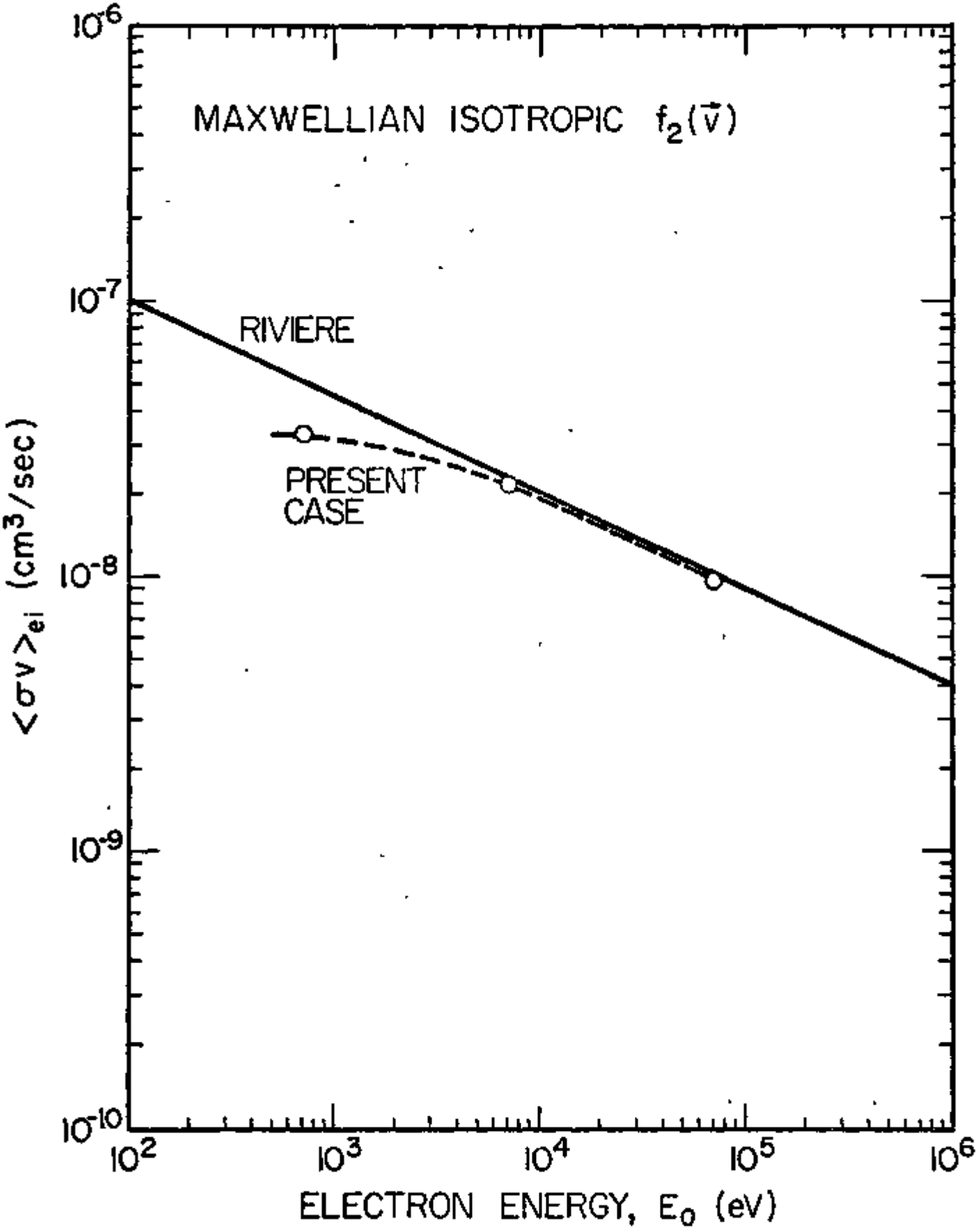
MAXWELLIAN ISOTROPIC $f_2(\vec{v})$
RIVIERE
PRESENT CASE
$\langle \sigma v \rangle_{ei}$ (cm^3/sec)
10^{-6}
10^{-7}
10^{-8}
10^{-9}
10^{-10}
10^2
10^3
10^4
10^5
10^6
ELECTRON ENERGY, E_0 (eV)

Figure 9

References

1. David J. Rose and Melville Clark, Jr., Plasmas and Controlled Fusion, (The MIT Press, Cambridge, Mass), 1961, p.80.

2. A. C. Riviere, "Penetration of Fast Hydrogen Atoms into a Fusion Reactor Plasma," Nuclear Fusion, 11, 363, (1971).

3. E. R. Salvatelli, G. Lantschner and W. Meckbach, "Search for a Possible Isotope Effect in Charge-Changing Collisions Involving Hydrogen and Deuterium," J. Phys. B. (Atom. Molec. Phys.), SER. 2, Vol. 2, 772, (1969).

4. J. P. Holdren, "Analytical Approximation to Collisional Distributions in Mirror Plasmas," Nuclear Fusion, 12, 267, (1972).

5. J. G. Cordey, Physics of Fluids, 14, 1407, (1971).

6. L. G. Kuo-Petravic, M. Petravic, and C. J. H. Watson, "Alpha-Particle Heating and the Energy Balance in a Mirror Reactor," B.N.E.S. Nuclear Fusion Reactor Conference, Culham Laboratory, Paper 2.4, 144, (September 1969).

7. An Engineering Design Study of a Reference Theta-Pinch Reactor (RTPR), LA-5336, ANL-8019, p. 10 ff., (March 1974).

8. T. H. Batzer, et al., "Conceptual Design of a Mirror Reactor for a Fusion Engineering Research Facility (FERF)," UCRL-51617, (28 August 1974).

9. Ronald L. Miller and George H. Miley, "Monte Carlo Simulation of Neutral Beam Injection into Fusion Reactors," submitted to Second International IEEE Conference on Plasma Science, Ann Arbor, Michigan, (May 1975).

10. G. A. Carlson and G. W. Hamilton, "Wall Bombardment Due to the Charge Exchange of Injected Neutrals with a Fusion Plasma," Lawrence Livermore Laboratory, Report No. UCRL-75306, 1974, also Proceedings of the First Topical Meeting on the Technology of Controlled Nuclear Fusion, AEC CONF.-740402-P1, 1974.